

Superconductivity in Two-Dimensional Systems with Unconventional Rashba Bands

Ran Wang,^{1,2} Jiayang Li,^{1,2} Xinliang Huang,^{1,2} Rui Song,^{3,1} and Ning Hao^{1,*}

¹*Anhui Province Key Laboratory of Low-Energy Quantum Materials and Devices,*

High Magnetic Field Laboratory, HFIPS, Chinese Academy of Sciences, Hefei, Anhui 230031, China

²*Science Island Branch of Graduate School, University of Science and Technology of China, Hefei, Anhui 230026, China*

³*Science and Technology on Surface Physics and Chemistry Laboratory, Mianyang, Sichuan 621908, China*

In two-dimensional system with Rashba spin-orbit coupling, it is well-known that superconductivity can have mixed spin-singlet and -triplet parity, and the \mathbf{d} -vector of spin-triplet pairing is parallel to \mathbf{g} -vector of Rashba spin-orbit coupling. Here, we propose a model to describe a two-dimensional system with unconventional Rashba bands and study its superconductivity. We show that the \mathbf{d} -vector of spin-triplet pairing can be either parallel or perpendicular to \mathbf{g} -vector of Rashba spin-orbit coupling depending on the different pairing interaction. We also propose a junction to generate tunneling current depending on the direction of \mathbf{d} -vector. It provides a detectable evidence to distinguish these two different but very similar pairing channels. Furthermore, we find this model can give arise to a subleading spin-singlet chiral p -wave topological superconducting state. More significantly, we find that such unconventional Rashba bands and unconventional superconducting pairings can be realized on surface of some superconducting topological materials, such as trigonal layered PtBi_2 .

Introduction-In systems characterized by two-dimensional (2D) geometry and Rashba spin-orbit coupling (SOC), the breaking of inversion symmetry leads to the lifting of spin degeneracy, resulting in superconductivity featuring a mixture of singlet and triplet pairings[1]. To achieve an equal superconducting transition temperature T_c as that of singlet pairing, the \mathbf{d} -vector for spin-triplet pairing is constrained to align parallel to the \mathbf{g} -vector associated with Rashba SOC[2]. These firmly established principles provide invaluable guidance for exploring unconventional superconductivity not only in complex noncentrosymmetric systems[3, 4], such as half-Heusler compounds[5–7] and transition metal dichalcogenides (TMDs)[8–10], but also in systems lacking local inversion centers[11–13], such as layered TMDs[14–16]. In two-band Rashba SOC model, the significance of Rashba SOC manifests in two key aspects. Firstly, it enables the two Fermi circles originating from two distinct bands to possess opposing chiral in-plane spin textures. Secondly, it mandates the alignment of the \mathbf{d} -vector for spin-triplet pairing to be parallel to it. These aspects are mutually consistent, leading to the conclusion that the \mathbf{g} -vector of Rashba SOC, the spin texture of the Fermi surface, and the \mathbf{d} -vector for spin-triplet pairing are all chiral. Nonetheless, some 2D systems exhibit unconventional Rashba bands[17–20], which is argued to originate from interband SOC[21], wherein the two Fermi circles from two distinct bands possess identical chiral in-plane spin textures, as depicted in Fig. 1(b). The immediate question that arises is the nature of the superconducting state in such 2D systems with unconventional Rashba bands.

In this work, we introduce a generic model which describe a 2D system with unconventional Rashba bands and can be realized in many material systems. The superconducting pairings can be categorized based on the

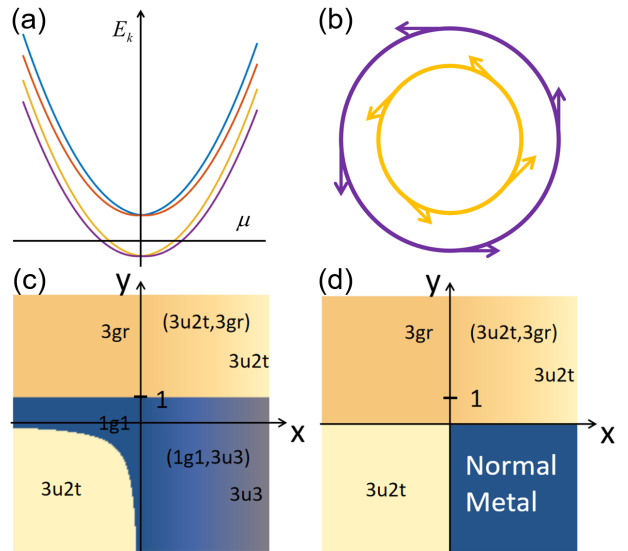


FIG. 1. (a) Energy dispersion of unconventional Rashba model. (b) Spin texture of unconventional Rashba bands with chemical potential show in (a). (c) The phase diagram of possible superconducting states without external magnetic field. (d) The phase diagram of superconducting states under strong external magnetic field. x, y are defined by $x = u_0/v_0 = u/v$ and $y = v/v_0 = u/u_0$. Here, v_0 (u_0) denotes intra-orbital (inter-orbital) pairing interaction in the zeroth order of k . v (u) denotes intra-orbital (inter-orbital) pairing interaction in the first order of k .

$SO(2)$ group. By solving the linearized gap function[2, 14], we identify both mixed singlet and triplet pairings. Specifically, we observe two competing spin-triplet pairings, one with its vector parallel and the other perpendicular to the Rashba SOC vector. The superconducting ground state is determined by the dominant pairing in-

teraction. The two spin-triplet pairings exhibit numerous similar properties. To differentiate between them, we propose a metal-superconductor junction. The tunneling currents may occur a tiny difference resulted by different quasi-particles of the states. Moreover, we examine the pairing breaking induced by the Zeeman effect and suggest that our model and associated findings could be realized on the surface of the trigonal-layered material PtBi_2 , which is recently reported to show exotic surface superconductivity[22].

Model-We start from a 4×4 Hamiltonian H_0 , that yields unconventional Rashba bands[23]. In the basis $\hat{\psi}_{\mathbf{k}} = (c_{\mathbf{k},1\uparrow}, c_{\mathbf{k},1\downarrow}, c_{\mathbf{k},2\uparrow}, c_{\mathbf{k},2\downarrow})^T$,

$$H_0(\mathbf{k}) = \xi_{\mathbf{k}}\sigma^0\tau^0 - \lambda_R(k_y\sigma^1 - k_x\sigma^2)(\tau^0 + \tau^1) + \lambda\sigma^3\tau^2. \quad (1)$$

Here, $i = 1, 2$ is for effective orbital or sublattice depending on the specific material while $\sigma = \uparrow, \downarrow$ denotes the spin in the annihilation operator $c_{\mathbf{k},i\sigma}$. Pauli matrices (σ^0, σ) and (τ^0, τ) span spin and orbital spaces respectively. $\xi_{\mathbf{k}} = tk^2 - \mu + \lambda$, the parameter t is for band curvature nearing Fermi surface. μ is chemical potential. λ_R describes intensity of Rashba SOC. λ stands for on-site SOC. For explicity, the vector of Rashba SOC is expressed as $\mathbf{g} = (-\hat{k}_y, \hat{k}_x, 0)$. We assume the two orbitals are connected to each other by a spatial inversion operation τ^1 , combining the operation $\mathbf{k} \rightarrow -\mathbf{k}$. Both the second and the third terms in Hamiltonian (1) break spatial inversion symmetry, the energy dispersion is straightforwardly obtained,

$$E_{N,\alpha\beta} = \xi_{\mathbf{k}} + \alpha\sqrt{\lambda^2 + \lambda_R^2 k^2} + \beta\lambda_R k \quad (2)$$

Here, $\alpha, \beta \in \{+, -\}$ labels band index. The spin texture for band α is $\mathbf{S}_{\alpha\beta} = \alpha(-k_y\mathbf{e}_x + k_x\mathbf{e}_y)\lambda_R/\sqrt{\lambda^2 + \lambda_R^2 k^2}$, which is along the tangential direction of Fermi circles for all of the four bands. The chirality of spin textures are the same for upper two bands and lower two bands independently while being opposite between upper and lower bands, since $\mathbf{S}_{\alpha\beta}$ is independent of β . We could get two Fermi circles with the same spin chirality if chemical potential lies in the band gap. This case correspond to unconventional Rashba bands in comparision with the conventional Rashba bands.

Pairing classification-Before solving superconductivity problem specifically, we give the superconducting pairing classification according to the symmetry of Hamiltonian (1). Superconducting pairs are expressed in the basis of creation and annihilation operators $(\hat{\psi}_{\mathbf{k}}, \hat{\psi}_{\mathbf{k}}^\dagger)$ as follows,

$$\begin{aligned} \hat{B}_{\mathbf{k}} &= (\hat{\psi}_{-\mathbf{k}})^T \mathcal{T}_{\Gamma}^\dagger(\mathbf{k}) \hat{\psi}_{\mathbf{k}}, \\ \hat{B}_{\mathbf{k}}^\dagger &= \hat{\psi}_{\mathbf{k}}^\dagger \mathcal{T}_{\Gamma}(\mathbf{k}) (\hat{\psi}_{-\mathbf{k}}^\dagger)^T. \end{aligned} \quad (3)$$

This form is useful in phenomenological theory of unconventional superconductivity[24–26]. It is convenient to devide the pairing matrix into two parts, $\mathcal{T}_{\Gamma}(\mathbf{k}) = \gamma(\mathbf{k})\mathcal{T}$,

TABLE I. $\phi_{g/u}$ and $\mathbf{d}_{g/u}$ are scalar and vector functions of k , respectively with g and u labeling even and odd under transformation $\mathbf{k} \rightarrow -\mathbf{k}$. The second column lists $\phi_{g/u}$ and $\mathbf{d}_{g/u}$ for simplest pairings to the lowest order of k , where $\hat{k}_x^2 + \hat{k}_y^2 = 1$ is normalized. The corresponding IRs for $SO(2)$ are listed in the third column, the same format of fonts denotes these pairings can be mixed. In the last column, we give every pairings a label for convienence, the first number denotes singlet or triplet in spin space and the letter g (u) means even (odd) of the whole pair under inversion transformation(See SMs[27] for details). The last letters label radial states (r), helical states (t) and out of plane states (p).

Pairing form	$\phi_{g/u} / \mathbf{d}_{g/u}$	IRs for $SO(2)$	Label
$i\phi_g\sigma^2\tau^0$	1	A	1g1
$i\phi_g\sigma^2\tau^1$	1	\mathbf{A}	1g2
$i\phi_g\sigma^2\tau^3$	1	\mathbb{A}	1u
$i\phi_u\sigma^2\tau^2$	$\hat{k}_x \pm i\hat{k}_y$	\mathcal{B}_{\pm}	1g3
$i(\mathbf{d}_u \cdot \boldsymbol{\sigma})\sigma^2\tau^0$	$(-\hat{k}_y, \hat{k}_x, 0)$	A	3u1t
	$(0, 0, \hat{k}_x \pm i\hat{k}_y)$	\mathcal{B}_{\pm}	3u1p
$i(\mathbf{d}_u \cdot \boldsymbol{\sigma})\sigma^2\tau^1$	$(\hat{k}_x, \hat{k}_y, 0)$	\mathbb{A}	3u2r
	$(-\hat{k}_y, \hat{k}_x, 0)$	\mathbf{A}	3u2t
$i(\mathbf{d}_u \cdot \boldsymbol{\sigma})\sigma^2\tau^3$	$(\hat{k}_x, \hat{k}_y, 0)$	A	3gr
	$(-\hat{k}_y, \hat{k}_x, 0)$	\mathbb{A}	3gt
$i(\mathbf{d}_g \cdot \boldsymbol{\sigma})\sigma^2\tau^2$	$(0, 0, 1)$	A	3u3

where \mathcal{T} is constructed by τ^μ in orbital space and describes the inversion operation, while $\gamma(\mathbf{k})$ is in spin space. We have taken the momentum dependence into $\gamma(\mathbf{k})$ by constructing it with power functions of k (basis functions of irreducible representations (IRs) for group $SO(3)$) and $\boldsymbol{\sigma}$ matrices. The pairings in different IRs for space group of the specific material would not be mixed, and the system with Hamiltonian(1) we study has symmetry of continuous rotation about z axis. Thus the irreducible pairings for group $SO(2)$ is obtained, listed in Table I, before consideration of mixed states. All IRs for $SO(2)$ are one dimensional with character in form of $e^{im\theta}$ ($m = 0, \pm 1, \pm 2, \dots$). We only consider the pairing in the zero and first order of k , i.e., $m = 0$ (IR A) and $|m| = 1$ (IR B_{\pm}).

Solutions for linear gap function-According to the phenomenological theory of superconductivity, the pairing interaction H_{int} can be expressed in a form of IRs of symmetry group of the system as follows,

$$H_{int} = - \sum_{\Gamma, j, \mathbf{k}, \mathbf{k}'} V_{\Gamma, j} c_{\mathbf{k}\mu}^\dagger (\mathcal{T}_{\Gamma, j})^{\mu\nu} c_{-\mathbf{k}\nu}^\dagger c_{-\mathbf{k}'\rho} (\mathcal{T}_{\Gamma, j}^\dagger)^{\rho\sigma} c_{\mathbf{k}'\sigma} \quad (4)$$

Indices μ, ν, ρ, σ count both orbital and spin degrees of freedom. j labels superconducting pairings of IR Γ , $V_{\Gamma, j}$ is the pairing parameter of j th channel in IR Γ . This interaction lead to a linearized gap equation.

$$\Delta_{\Gamma, j} = V_{\Gamma, j} \sum_l \chi_{\Gamma, jl} \Delta_{\Gamma, l}. \quad (5)$$

$\Delta_{\Gamma, j} = -V_{\Gamma, j} \sum_{\mathbf{k}\mu\nu} \langle c_{-\mathbf{k}\mu} (\mathcal{T}_{\Gamma, j}^\dagger)^{\mu\nu} c_{\mathbf{k}\nu} \rangle$ is the supercon-

ducting order parameter; $\chi_{\Gamma,jl}$ is defined as superconductivity susceptibility between j and l pairings of IR Γ .

$$\chi_{\Gamma,jl} = \frac{1}{\beta} \sum_{n,\mathbf{k}} \text{Tr}[\mathcal{T}_{\Gamma,j}^{\dagger}(\mathbf{k}) G^0(\mathbf{k}, i\omega_n) \mathcal{T}_{\Gamma,l}(\mathbf{k}) (G^0(-\mathbf{k}, -i\omega_n))^T] \quad (6)$$

Here, $G^0(\mathbf{k}, i\omega_n)$ is the Matsubara Green function for normal state (See Supplementary Materials (SMs)[27] for details), $\beta = 1/k_B T$. One could examine the mixing of states from linearized gap equation (5) and obtain critical temperatures. Here, we consider the unconventional Rashba bands case with chemical potential lying in the gap between upper two and lower two bands, as shown in Fig. 1(a). $V_{\Gamma,j}$ could be different between singlet and triplet pairings as well as intra- and inter-orbital pairings, while is identical for pairings with the same order of momentum k_i . Thus, we import four interaction parameters $V_{\Gamma,j}$: v_0 for 1g1 and 1u; u_0 for 1g2 and 3u3; v for 3u1 and 3g; u for 1g3 and 3u2, and keep in mind that negative $V_{\Gamma,j}$ would cause zero order parameter $\Delta_{\Gamma,j}$.

From the solutions of Eq. (5), there are four types of separately mixed states: a $\in\{1g1, 3u1t, 3u3\}$; b $\in\{1g2, 3u2t, 3gr\}$; c $\in\{1u, 3u2r, 3gt\}$; d $\in\{1g3, 3u1t\}$, each of them is connected to a same critical temperature decided by the linearized gap equation Eq.(5) (See SMs[27] for explicit relations). We get the phase diagram Fig. 1(c) by comparing these T_c s.

Properties of possible pairings—The four possible pairings have very different properties. 1g1 pairing is a standard spin-singlet pairing, and 3u3 pairing is a k -independent spin-triplet pairing. Both of them can be mixed together. 3u2t and 3gr pairings have more interesting property. Both pairings give topological superconducting states characterized by a $Z_2 = 1$ number. Their bulk dispersion and edge spectrum are similar, as shown in Fig. 2 (a). Besides such same properties and their ability for mixture, their \mathbf{d} -vectors are very different, that $\mathbf{d}_{3u2t} \parallel \mathbf{g}$ and $\mathbf{d}_{3gr} \perp \mathbf{g}$. Remarkably, the 1g3 pairing gives a spin-singlet chiral p -wave topological superconducting state due to the time-reversal symmetry breaking. Such topological superconducting state can be characterized by a Chern number of $C = \pm 2$, its bulk dispersion and edge spectrum are shown in Fig. 2 (b). The 1g3 pairing is subleading and does not appear in the phase diagram. However, its T_c is comparable to leading pairing from linear gap function calculation. It is still possible due to the complicated parameters in real materials. The Zeeman effect induced by an external magnetic field offers a valuable means to distinguish between pairings in different spin states [2, 4, 10]. The pairs exhibits greater sensitivity to out-of-plane fields due to the higher order pair-breaking terms introduced by in-plane fields, which is consistent with Ref.[28]. Additionally, the symmetry preserved under an out-of-plane magnetic field enables the solvability of the revised linear gap function (refer to SMs[27] for details). It is observed that both the

3u2t and 3gr pairings remain unaffected, whereas pairings 1g1 and 3u3 can be suppressed by an out-of-plane magnetic field. The revised phase diagram under magnetic field conditions is illustrated in Fig. 1(d).

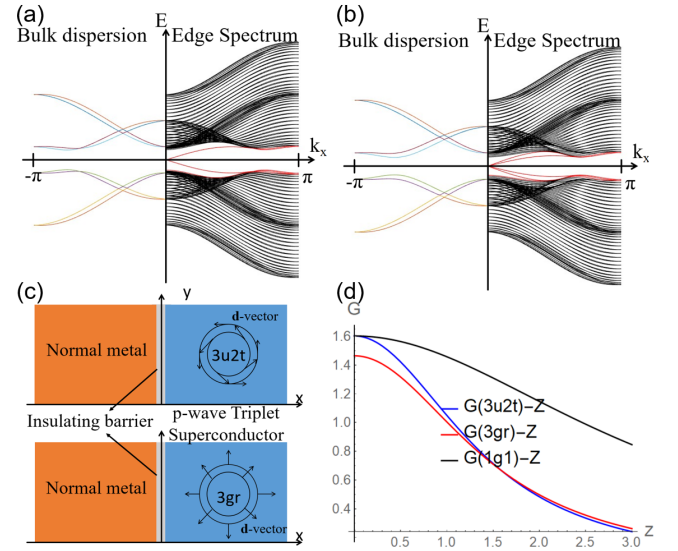


FIG. 2. (a) Bulk (edge) quasiparticle dispersion (spectrum) for the superconducting states with 3u2t pairing. The plotting is similar for 3gr pairing. (b) Bulk (edge) quasiparticle dispersion (spectrum) for the superconducting states with 1g3 pairing. (c) Schematic diagram of a junction including a normal metal and a p-wave triplet unconventional Rashba superconductor. The superconducting state has either 3u2t pairing or 3gr pairing. (d) Plot of G as function as Z for three types of junctions. Here, $Z = 2mU_0/h^2k_F$. Parameters: $\lambda_Rk_F/2\lambda = 0.2$, $\Delta/E = 0.95$.

Whether with or without magnetic field, the two 3u2t and 3gr pairings could be pure or mixed near T_c , depending on the relative magnitude between the two interaction parameters u and v . Governed by the same topological property and T_c -magnetic field response, the difference of these two states is hard to be detected by experiments. Fortunately, the energy dispersions of quasi-particles are not exactly the same Eq.(7),(8), which provides opportunity to distinguish them.

$$E_{S,\alpha\beta}^{3u2t} = \pm \sqrt{\left(\xi_{\mathbf{k}} + \alpha \sqrt{\lambda^2 + \lambda_R^2 k^2} + \beta \lambda_R k \right)^2 + \Delta^2} \quad (7)$$

$$E_{S,\alpha\beta}^{3gr} = \pm \sqrt{\left(\alpha \sqrt{\lambda^2 + \lambda_R^2 k^2} + f_{\beta} \right)^2 + \Delta^2 \cos^2 \phi} \quad (8)$$

Here, $\alpha, \beta \in \{+, -\}$, being the same as normal states (2). $\phi = \arctan(\lambda_R k / \lambda)$, $f_{\beta} = \sqrt{(\xi_{\mathbf{k}} + \beta \lambda_R k)^2 + \Delta^2 \sin^2 \phi}$. Superconducting order parameter Δ is setted to be a constant. We propose a normal metal-superconductor junction [29–31] in the $x-y$ plane, with a barrier at $x = 0$ to separate the two regions. This junction is schemati-

cally illustrated in Fig. 2 (c). Normal metal lies in the region $x < 0$, while in the region where $x > 0$, it is the unconventional Rashba system with superconducting states of 3u2t or 3gr. We find a conductance difference results from the tiny difference between the quasi-particle energy of the two states. To show this physics without formidable calculation, we use an effective Hamiltonian for the lower two bands (See SMs[27] for details). And the Hamiltonian to describe the junction is written as

$$H_t = (\xi_k - \lambda)\sigma^0\eta^3\Theta(-x) + \hat{H}_{BdG}^{eff}\Theta(x) + U_0\sigma^0\eta^3\delta(x) \quad (9)$$

Here Pauli matrices (η^0, η) span the particle-hole space. ξ_k is the same as that in Hamiltonian (1), being a simplified parabolic dispersion. U_0 is the barrier potential. For simplicity, we have also set both effective mass and chemical potential to be equal for the whole junction. $\delta(x)$ is delta function and $\Theta(x)$ is step function. The Hamiltonian in Eq.(9) can be solved under the continuity condition of wave function at the interface (See SMs[27] for details), then one get tunneling conductance of the junction. The conductance as functions of the barrier intensity are plotted in Fig. 2(d). At a zero barrier limit $Z = 0$, We find the conductance of 3u2t state is the same as that of the standard singlet pairing 1g1, meanwhile it is larger than the conductance of 3gr. The conductance difference is

$$\delta G \approx \left(\frac{\lambda_R k_F}{2\lambda} \right)^2 \frac{\Delta^2}{E\sqrt{E^2 - \Delta^2}} \quad (10)$$

which can help the experiments to distinguish these two different unconventional pairings.

Material realization-We propose that such unconventional Rashba bands can be realized on the surface of a trigonal layered PtBi_2 compound. In our previous work[32], we confirmed trigonal layered PtBi_2 tends to form the buckled structure for the top Bi layer, as shown in Fig. 3 (a)-(b). This structure naturally breaks the centrosymmetry and possesses large Rashba SOC. The calculations in Fig. 3 (c) show that Pt cleavage surface bands have large spin-splitting feature, and the spin texture for given doping shows the clear properties of aforementioned unconventional Rashba bands. More intriguingly, this compound is recently found to be a superconductor below a temperature of several Kelvin[28, 33]. Thus, the surface unconventional Rashba bands also fall into the superconducting states through either bulk-surface proximity effect or the effective surface pairing interaction. Recent experiment observed some interesting phenomena[22, 34, 35], which is relevant to the surface superconductivity. In our case, the unconventional Rashba bands can be realized by the finite tuning the doping level through the neighbor element replacement.

Conclusion-In summary, we present an unconventional Rashba band model that deviates substantially from the conventional Rashba model. We demonstrate that the

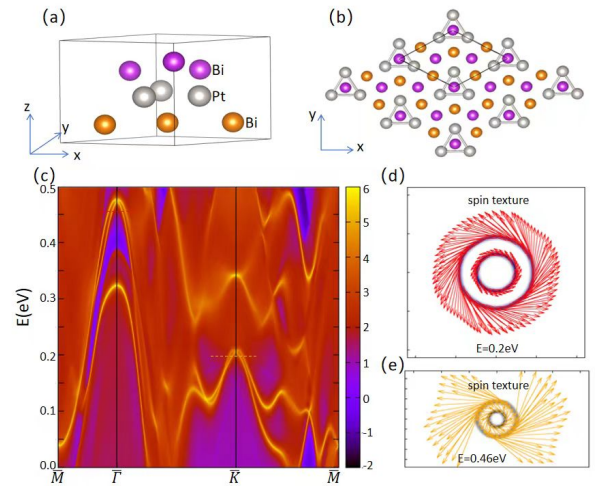


FIG. 3. (a)-(b) The crystalline structure of trigonal layered PtBi_2 . The top Bi layer form buckled structure and break the inverson symmetry. (c) The Pt cleavage surface spectrum calculated from a slab geometry. The plotting is along the high-symmetry line in the reduced surface Brillouin zone. (d)-(e) The spin texture for the two Fermi circles with given doping levels shown in (c).

\mathbf{d} -vector of spin-triplet pairing in our model can align either parallel or perpendicular to the \mathbf{g} -vector of Rashba spin-orbit coupling, contingent upon different pairing interactions. This discovery updates the established notion that the \mathbf{d} -vector must align parallel to the \mathbf{g} -vector in two-dimensional systems with Rashba spin-orbit coupling. Furthermore, we propose an experimentally feasible junction to discern and differentiate between the two distinct types of spin-triplet superconducting states with varying \mathbf{d} -vectors. Notably, some material systems exhibit such unconventional Rashba bands, with the trigonal layered PtBi_2 being a promising candidate. Our investigation provides new understandings for studying unconventional superconductivity in non-centrosymmetric materials with unconventional band structures.

We thank Prof. Songbo Zhang for helpful discussions. This work was financially supported by the National Key R&D Program of China (Grants No. 2022YFA1403200), National Natural Science Foundation of China (Grants No. 92265104, No. 12022413, No. 11674331), the Basic Research Program of the Chinese Academy of Sciences Based on Major Scientific Infrastructures (Grant No. JZHKYPT-2021-08), the CASHIPS Director's Fund (Grant No. BJPY2023A09), the "Strategic Priority Research Program (B)" of the Chinese Academy of Sciences (Grant No. XDB33030100), and the Major Basic Program of Natural Science Foundation of Shandong Province (Grant No. ZR2021ZD01). A portion of this work was supported by the High Magnetic Field Laboratory of Anhui Province, China.

* haon@hmfl.ac.cn

[1] L. P. Gor'kov and E. I. Rashba, Superconducting 2d system with lifted spin degeneracy: Mixed singlet-triplet state, *Phys. Rev. Lett.* **87**, 037004 (2001).

[2] P. A. Frigeri, D. F. Agterberg, A. Koga, and M. Sigrist, Superconductivity without inversion symmetry: MnSi versus CePt_3Si , *Phys. Rev. Lett.* **92**, 097001 (2004).

[3] M. Zeng, D.-H. Xu, Z.-M. Wang, and L.-H. Hu, Spin-orbit coupled superconductivity with spin-singlet nonunitary pairing, *Phys. Rev. B* **107**, 094507 (2023).

[4] X. Xi, Z. Wang, W. Zhao, J.-H. Park, K. T. Law, H. Berger, L. Forró, J. Shan, and K. F. Mak, Ising pairing in superconducting nbse2 atomic layers, *Nature Physics* **12**, 139 (2016).

[5] I. Boettcher and I. F. Herbut, Superconducting quantum criticality in three-dimensional luttinger semimetals, *Phys. Rev. B* **93**, 205138 (2016).

[6] J. W. F. Venderbos, L. Savary, J. Ruhman, P. A. Lee, and L. Fu, Pairing states of spin- $\frac{3}{2}$ fermions: Symmetry-enforced topological gap functions, *Phys. Rev. X* **8**, 011029 (2018).

[7] M. Bahari, S.-B. Zhang, and B. Trauzettel, Intrinsic finite-energy cooper pairing in $j = 3/2$ superconductors, *Phys. Rev. Res.* **4**, L012017 (2022).

[8] N. F. Q. Yuan, K. F. Mak, and K. T. Law, Possible topological superconducting phases of mos₂, *Phys. Rev. Lett.* **113**, 097001 (2014).

[9] B. T. Zhou, N. F. Q. Yuan, H.-L. Jiang, and K. T. Law, Ising superconductivity and majorana fermions in transition-metal dichalcogenides, *Phys. Rev. B* **93**, 180501 (2016).

[10] Y. Saito, Y. Nakamura, M. S. Bahramy, Y. Kohama, J. Ye, Y. Kasahara, Y. Nakagawa, M. Onga, M. Tokunaga, T. Nojima, Y. Yanase, and Y. Iwasa, Superconductivity protected by spin-valley locking in ion-gated mos₂, *Nature Physics* **12**, 144 (2016).

[11] M. H. Fischer, F. Loder, and M. Sigrist, Superconductivity and local noncentrosymmetry in crystal lattices, *Phys. Rev. B* **84**, 184533 (2011).

[12] J. Goryo, M. H. Fischer, and M. Sigrist, Possible pairing symmetries in srptas with a local lack of inversion center, *Phys. Rev. B* **86**, 100507 (2012).

[13] M. H. Fischer, M. Sigrist, D. F. Agterberg, and Y. Yanase, Superconductivity and local inversion-symmetry breaking, *Annual Review of Condensed Matter Physics* **14**, 153 (2023), <https://doi.org/10.1146/annurev-conmatphys-040521-042511>.

[14] C.-X. Liu, Unconventional superconductivity in bilayer transition metal dichalcogenides, *Phys. Rev. Lett.* **118**, 087001 (2017).

[15] G.-W. Qiu and Y. Zhou, Inhomogeneous superconducting states in two weakly linked superconducting ultrathin films, *Phys. Rev. B* **105**, L100506 (2022).

[16] N. F. Q. Yuan, Orbital fulde-ferrell-larkin-ovchinnikov state in an ising superconductor, *Phys. Rev. Res.* **5**, 043122 (2023).

[17] H. Mirhosseini, J. Henk, A. Ernst, S. Ostanin, C.-T. Chiang, P. Yu, A. Winkelmann, and J. Kirschner, Unconventional spin topology in surface alloys with rashba-type spin splitting, *Phys. Rev. B* **79**, 245428 (2009).

[18] F. Meier, V. Petrov, S. Guerrero, C. Mudry, L. Patthey, J. Osterwalder, and J. H. Dil, Unconventional fermi surface spin textures in the $\text{bi}_x\text{pb}_{1-x}/\text{Ag}(111)$ surface alloy, *Phys. Rev. B* **79**, 241408 (2009).

[19] C. Mera Acosta, O. Babilonia, L. Abdalla, and A. Fazzio, Unconventional spin texture in a noncentrosymmetric quantum spin hall insulator, *Phys. Rev. B* **94**, 041302 (2016).

[20] I. A. Nechaev and E. E. Krasovskii, Spin polarization by first-principles relativistic $\mathbf{k} \cdot \mathbf{p}$ theory: Application to the surface alloys pbag_2 and biag_2 , *Phys. Rev. B* **100**, 115432 (2019).

[21] H. Bentmann, S. Abdelouahed, M. Mulazzi, J. Henk, and F. Reinert, Direct observation of interband spin-orbit coupling in a two-dimensional electron system, *Phys. Rev. Lett.* **108**, 196801 (2012).

[22] A. Kuibarov, O. Suvorov, R. Vocaturo, A. Fedorov, R. Lou, L. Merkwitz, V. Voroshnin, J. I. Facio, K. Koepernik, A. Yaresko, G. Shipunov, S. Aswartham, J. v. d. Brink, B. Büchner, and S. Borisenko, Evidence of superconducting fermi arcs, *Nature* **626**, 294 (2024).

[23] X. Huang, Y. Xiao, R. Song, and N. Hao, A generic model with unconventional rashba bands and giant spin galvanic effect (2024), [arXiv:2403.04155 \[cond-mat.mes-hall\]](https://arxiv.org/abs/2403.04155).

[24] M. Sigrist and K. Ueda, Phenomenological theory of unconventional superconductivity, *Rev. Mod. Phys.* **63**, 239 (1991).

[25] R. Konno and K. Ueda, Superconductivity and antiferromagnetism in heavy-electron systems, *Phys. Rev. B* **40**, 4329 (1989).

[26] K. Ueda and T. M. Rice, p-wave superconductivity in cubic metals, *Phys. Rev. B* **31**, 7114 (1985).

[27] Supplementary materials.

[28] A. Veyrat, V. Labracherie, D. L. Bashlakov, F. Cagliari, J. I. Facio, G. Shipunov, T. Charvin, R. Acharya, Y. Naidyuk, R. Giraud, J. van den Brink, B. Büchner, C. Hess, S. Aswartham, and J. Dufouleur, Berezinskii-kosterlitz-thouless transition in the type-i weyl semimetal ptbi₂, *Nano Letters* **23**, 1229 (2023), pMID: 36720048, <https://doi.org/10.1021/acs.nanolett.2c04297>.

[29] Q. Cheng, B. Jin, and H. Ma, Orientation-dependent conductance in 2deg/spin-triplet superconductor junctions with rashba spin-orbit coupling, *Physica B: Condensed Matter* **478**, 52 (2015).

[30] B. Lv, C. Zhang, and Z. Ma, Specular andreev reflection in the interface of a two-dimensional semiconductor with rashba spin-orbit coupling and a d-wave superconductor, *Phys. Rev. Lett.* **108**, 077002 (2012).

[31] L. Majidi and R. Asgari, Specular andreev reflection in thin films of topological insulators, *Phys. Rev. B* **93**, 195404 (2016).

[32] W. Gao, X. Zhu, F. Zheng, M. Wu, J. Zhang, C. Xi, P. Zhang, Y. Zhang, N. Hao, W. Ning, and M. Tian, A possible candidate for triply degenerate point fermions in trigonal layered ptbi₂, *Nature Communications* **9**, 3249 (2018).

[33] G. Shipunov, I. Kovalchuk, B. R. Piening, V. Labracherie, A. Veyrat, D. Wolf, A. Lubk, S. Subakti, R. Giraud, J. Dufouleur, S. Shokri, F. Cagliari, C. Hess, D. V. Efremov, B. Büchner, and S. Aswartham, Polymorphic ptbi₂: Growth, structure, and superconducting properties, *Phys. Rev. Mater.* **4**, 124202 (2020).

[34] J. Zabala, P. Pedrazzini, F. J. Castro, and V. F. Correa, Enhanced weak superconductivity in trigonal γ -ptbi₂

(2023), [arXiv:2309.00105 \[cond-mat.supr-con\]](https://arxiv.org/abs/2309.00105).
[35] S. Schimmel, Y. Fasano, S. Hoffmann, J. Puig, G. Shipunov, D. Baumann, S. Aswartham, B. Büchner, and C. Hess, High-*tc* surface superconductivity in topological weyl semimetal t-ptbi2 (2023), [arXiv:2302.08968 \[cond-mat.supr-con\]](https://arxiv.org/abs/2302.08968).

I. CLASSIFICATION OF SUPERCONDUCTING PAIRS

We claim in the main text that the pairing matrix is divided into two parts, $\mathcal{T}_\Gamma(\mathbf{k}) = \gamma(\mathbf{k})\mathcal{T}$. Here we are going to elaborate the whole pair parity under inversion based on the character of \mathcal{T} . In our assumption of two obitals being spacial inversion, one should replace the field $c_{i\sigma}^\dagger(\mathbf{k})$ by $c_{3-i,\sigma}^\dagger(-\mathbf{k})$ as taking inversion operation, which is equivalent to the transformation on the matrices $\gamma(\mathbf{k})\mathcal{T}_{ij} \rightarrow -\gamma^T(\mathbf{k})(\mathcal{T}^T)_{3-i,3-j}$ or $\gamma(\mathbf{k})\mathcal{T} \rightarrow -\gamma^T(\mathbf{k})\tau^1\mathcal{T}^*\tau^1$. Since one could get different parity under other assumptions, the labels we use may be changed. However in the context of inversion symmetry breaking, states are not selected by parity, thus the labels has little significance to do with the main results of this letter.

II. MATSUBARA GREEN FUNCTION

The unitary transformation matrix U diagonalizes normal state Hamiltonian H_0 (Eq.(1) in the main text)

$$U^{-1}H_0U = \begin{pmatrix} E_{++} & & & \\ & E_{+-} & & \\ & & E_{-+} & \\ & & & E_{--} \end{pmatrix} \quad (11)$$

We choose one explicit form

$$U = \frac{1}{2}[1 - i\sin\theta\cos\phi\sigma^1 + i\cos\theta\cos\phi\sigma^2 + i\cos\theta\sigma^1\tau^1 + i\sin\theta\sigma^2\tau^1 + i\cos\phi\sigma^3\tau^1 - i\sin\phi\sigma^3\tau^2 - \sin\theta\sin\phi\sigma^1\tau^3 + \cos\theta\sin\phi\sigma^2\tau^3] \quad (12)$$

where $\theta = \arctan(k_y/k_x)$, $\phi = \arctan(\lambda_R k/\lambda)$. The Matsubara Green function for normal state electrons is

$$G^0(\mathbf{k}, i\omega_n) = U\tilde{G}(\mathbf{k}, i\omega_n)U^{-1} \quad (13)$$

here \tilde{G} is Green function for the eigenstates, $\omega_n = (2n + 1)\pi/\beta$.

$$\tilde{G}(\mathbf{k}, i\omega_n) = \frac{1}{4} \sum_{\alpha, \beta} \tilde{G}_{\alpha\beta}(\mathbf{k}, i\omega_n) (\sigma^0 + \beta\sigma^3) \otimes (\tau^0 + \alpha\tau^3) \quad (14)$$

$$\tilde{G}_{\alpha\beta}(\mathbf{k}, i\omega_n) = \frac{1}{i\omega_n - E_{\alpha\beta}} \quad (15)$$

Then we get Green function for normal state

$$G^0(\mathbf{k}, i\omega_n) = G_{++++}\sigma^0\tau^0 + G_{+---}[\frac{\lambda_R k}{\sqrt{\lambda^2 + \lambda_R^2 k^2}}(\hat{\mathbf{k}} \times \boldsymbol{\sigma})_z\tau^0 + \frac{\lambda}{\sqrt{\lambda^2 + \lambda_R^2 k^2}}\sigma^3\tau^2] + G_{+-+-}(\hat{\mathbf{k}} \times \boldsymbol{\sigma})_z\tau^1 + G_{--+-}[\frac{\lambda_R k}{\sqrt{\lambda^2 + \lambda_R^2 k^2}}\sigma^0\tau^1 - \frac{\lambda}{\sqrt{\lambda^2 + \lambda_R^2 k^2}}(\hat{\mathbf{k}} \cdot \boldsymbol{\sigma})\tau^3] \quad (16)$$

where $G_{\alpha\beta\gamma\delta} = (\alpha\tilde{G}_{++} + \beta\tilde{G}_{+-} + \gamma\tilde{G}_{-+} + \delta\tilde{G}_{--})/4$.

III. SUPERCONDUCTIVITY SUSCEPTIBILITY

The calculation of superconductivity susceptibilities(Eq.(6) in the main text) involves Sumation in momentum space, which is handled in the conventional way of changing into integral in energy $\sum_{\mathbf{k}} \rightarrow \frac{1}{2\pi} N \int d\Omega \int d\epsilon$. N is DOS for each band and $d\Omega$ is the infinitesimal solid angle of 2D. The general results for $\frac{d}{d\Omega} [\frac{1}{\beta} \sum_{n,\mathbf{k}} G(\mathbf{k}, i\omega_n) G'(-\mathbf{k}, -i\omega_n)]$ are

$$\frac{d}{d\Omega} \left[-\frac{1}{\beta} \sum_{n,\mathbf{k}} \frac{1}{i\omega_n - \epsilon_k} \frac{1}{i\omega_n + \epsilon_k} \right] = N \int_{-\omega_D}^{+\omega_D} d\epsilon \frac{\tanh \frac{\beta\epsilon}{2}}{2\epsilon} = N \ln \frac{2e^\gamma \omega_D}{\pi k_B T} \equiv \frac{1}{N_B} \chi_0 \quad (17)$$

$$\frac{d}{d\Omega} \left[-\frac{1}{\beta} \sum_{n,\mathbf{k}} \frac{1}{i\omega_n - \epsilon_k + x} \frac{1}{i\omega_n + \epsilon_k + y} \right] = \begin{cases} [\frac{1}{N_B} \chi_0 + N\mathcal{C}_0(T, \frac{x+y}{2})], & (|x|, |y| \ll \omega_D) \\ 0, & (others) \end{cases} \quad (18)$$

ϵ_k is energy measured from Fermi surface, ω_D is Debye frequency. $\mathcal{C}_0(T, x) = \text{Re}[\psi^{(0)}(\frac{1}{2}) - \psi^{(0)}(\frac{1}{2} + i\frac{x}{2\pi k_B T})]$, where $\psi^{(0)}(z)$ is the di-gamma function. N_B is the number of bands near Fermi surface, only which contribute to superconductivity. χ_0 is the superconductivity susceptibility for the spin singlet state in standard Bardeen-Cooper-Schrieffer (BCS) theory of 2D. We assume the Rashba SOC is relatively weak compared to the on-site one ($\lambda_R k_F \ll \lambda$), meanwhile let Fermi surface to stay in the gap of upper and lower bands for the simplicity. Define the notation $g_{\mu\nu\rho\sigma}^{\alpha\beta\gamma\delta} = \frac{d}{d\Omega} [\frac{1}{\beta} \sum_{n,\mathbf{k}} G_{\alpha\beta\gamma\delta}(\mathbf{k}, i\omega_n) G_{\mu\nu\rho\sigma}(-\mathbf{k}, -i\omega_n)]$, whose results are

$$g_{++++}^{++++} = g_{++--}^{++--} = -g_{+++-}^{+++-} = -g_{+-+-}^{+-+-} = \frac{1}{8} \chi_0 + \frac{1}{8} N\mathcal{C}_0(T, \lambda_R k_F) \quad (19)$$

$$g_{+-+-}^{+-+-} = g_{+--+}^{+--+} = -g_{+-+-}^{+-+-} = -g_{+-+-}^{+-+-} = -\frac{1}{8} N\mathcal{C}_0(T, \lambda_R k_F) \quad (20)$$

$g_{\mu\nu\rho\sigma}^{\alpha\beta\gamma\delta}$ s not listed above are zero. Since we are discussing about pairings to the first order of k and there is dependence of $\hat{k}_i = k_i/|\mathbf{k}|(i = x, y, z)$ in Eq. (16), one could concern about the summations in form of $\frac{1}{\beta} \sum_{n,\mathbf{k}} k_i k_j G(\mathbf{k}, i\omega_n) G'(-\mathbf{k}, -i\omega_n)$, etc. However the $\hat{\mathbf{k}}$ dependence will just goes into solid angle integral provided pairings are normalized, thus we will use superconductivity susceptibility in differential sense $\tilde{\chi}_{\Gamma,ij} = d\chi_{\Gamma,ij}/d\Omega$ for convenience.

A. Singlet states:

$$\chi_{1g1,1g1} = \chi_0 \quad (21)$$

$$\chi_{1g1,1g2} = \chi_{1g2,1g1} = 0 \quad (22)$$

$$\chi_{1g2,1g2} = \frac{\lambda_R^2 k^2}{\lambda^2 + \lambda_R^2 k^2} \chi_0 \quad (23)$$

$$\chi_{1u,1u} = \frac{\lambda_R^2 k^2}{\lambda^2 + \lambda_R^2 k^2} (\chi_0 + 2N\mathcal{C}_0(T, \lambda_R k_F)) \quad (24)$$

$$\chi_{1u,1g1} = \chi_{1g1,1u} = \chi_{1u,1g2} = \chi_{1g2,1u} = 0 \quad (25)$$

$$\tilde{\chi}_{1g3,1g3} = |\phi_1|^2 [\chi_0 + 2N\mathcal{C}_0(T, \lambda_R k_F)] \quad (26)$$

1g1 and 1g2 correspond to A_g representation for group $SO(2)$, while 1u correspond to A_u . 1g3 is the first $\hat{k}_i(i = x, y, z)$ dependent pairing, which corresponds to $B_{\pm,g}$ representation, however the two independent normalized factors $\phi_1 = \hat{k}_x \pm i\hat{k}_y$ contributing to a factor 1 in solid angle integral make $\chi_{1g3,1g3}$ no more than $g_{\mu\nu\rho\sigma}^{\alpha\beta\gamma\delta}$ s.

B. Triplet states:

Calculations all depend on solid angle integral for triplet states. Wirte $\tilde{\chi}$ in form of $\tilde{\chi}_0 + \Delta\tilde{\chi}$, $\Delta\tilde{\chi}$ is the pair breaking term which describes the deviation of critical temperature from T_{c0} . $\Delta\tilde{\chi}$ is always minimized by radial($\mathbf{d} \parallel \hat{\mathbf{k}}$),

helical($\mathbf{d} \perp \hat{\mathbf{k}}$), or out of plane($\mathbf{d}_{\parallel} = 0$) superconducting states. Therefore the states we focus on have maximum superconductivity susceptibilities and are independent of integral in solid angle. The helical state(3u1t) gives out an A_u representation, while the out of plane state(3u1p) is a $B_{\pm,u}$ representation.

$$\begin{aligned} \tilde{\chi}_{3u1,3u1} &= \frac{\lambda_R^2 k_F^2}{\lambda^2 + \lambda_R^2 k_F^2} (|\mathbf{d}_{\parallel}|^2 - |\mathbf{d} \cdot \hat{\mathbf{k}}|^2) \chi_0 + \frac{\lambda^2}{\lambda^2 + \lambda_R^2 k_F^2} |\mathbf{d}_{\perp}|^2 (\chi_0 + 2N\mathcal{C}_0(T, \lambda_R k_F)) \\ &\rightarrow \begin{cases} \chi_{3u1t,3u1t} = \frac{\lambda_R^2 k_F^2}{\lambda^2 + \lambda_R^2 k_F^2} \chi_0 & \mathbf{d} = (-\hat{k}_y, \hat{k}_x, 0) \\ \chi_{3u1p,3u1p} = \frac{\lambda^2}{\lambda^2 + \lambda_R^2 k_F^2} (\chi_0 + 2N\mathcal{C}_0(T, \lambda_R k_F)) & \mathbf{d} = (0, 0, \hat{k}_x \pm i\hat{k}_y) \end{cases} \end{aligned} \quad (27)$$

3u2 is divided to a radial state(3u2r) and a helical state(3u2t), both of which are A_u representations for group $SO(2)$.

$$\begin{aligned} \tilde{\chi}_{3u2,3u2} &= \left(\frac{\lambda^2}{\lambda^2 + \lambda_R^2 k_F^2} |\mathbf{d}_{\parallel}|^2 + \frac{\lambda_R^2 k^2}{\lambda^2 + \lambda_R^2 k_F^2} (|\mathbf{d}_{\parallel}|^2 - |\mathbf{d} \cdot \hat{\mathbf{k}}|^2) \right) \chi_0 + \frac{\lambda^2}{\lambda^2 + \lambda_R^2 k_F^2} |\mathbf{d} \cdot \hat{\mathbf{k}}|^2 2N\mathcal{C}_0(T, \lambda_R k_F) \\ &\rightarrow \begin{cases} \chi_{3u2r,3u2r} = \frac{\lambda^2}{\lambda^2 + \lambda_R^2 k_F^2} (\chi_0 + 2N\mathcal{C}_0(T, \lambda_R k_F)) & \mathbf{d} = (\hat{k}_x, \hat{k}_y, 0) \\ \chi_{3u2t,3u2t} = \chi_0 & \mathbf{d} = (-\hat{k}_y, \hat{k}_x, 0) \end{cases} \end{aligned} \quad (28)$$

There are also two channels in 3g, radial state(3gr) and helical state(3gt), both of them are A_g representation.

$$\begin{aligned} \tilde{\chi}_{3g,3g} &= \frac{\lambda^2}{\lambda^2 + \lambda_R^2 k_F^2} |\mathbf{d}_{\parallel}|^2 \chi_0 + (|\mathbf{d}_{\parallel}|^2 - |\mathbf{d} \cdot \hat{\mathbf{k}}|^2) \left(\frac{\lambda_R^2 k^2}{\lambda^2 + \lambda_R^2 k_F^2} \chi_0 + 2N\mathcal{C}_0(T, \lambda_R k_F) \right) \\ &\rightarrow \begin{cases} \chi_{3gr,3gr} = \frac{\lambda^2}{\lambda^2 + \lambda_R^2 k_F^2} \chi_0 & \mathbf{d} = (\hat{k}_x, \hat{k}_y, 0) \\ \chi_{3gt,3gt} = \chi_0 + 2N\mathcal{C}_0(T, \lambda_R k_F) & \mathbf{d} = (-\hat{k}_y, \hat{k}_x, 0) \end{cases} \end{aligned} \quad (29)$$

In the zeroth order, the only possible vector function for 3u3 is $\mathbf{d} = (0, 0, 1)$, which is for A_u representation.

$$\begin{aligned} \tilde{\chi}_{3u3,3u3} &= \frac{\lambda^2}{\lambda^2 + \lambda_R^2 k_F^2} |\mathbf{d}_{\perp}|^2 \tilde{\chi}_0 + \frac{\lambda_R^2 k^2}{\lambda^2 + \lambda_R^2 k_F^2} (|\mathbf{d}_{\parallel}|^2 - |\mathbf{d} \cdot \hat{\mathbf{k}}|^2) (\tilde{\chi}_0 + 2N\mathcal{C}_0(T, \lambda_R k_F)) \\ &\rightarrow \chi_{3u3,3u3} = \frac{\lambda^2}{\lambda^2 + \lambda_R^2 k_F^2} \chi_0 \end{aligned} \quad (30)$$

The possible combinations between Singlets and Triplet states are: ①A: 1g1, 1g2, 1u, 3u1t, 3u2r, 3u2t, 3gr, 3gt, 3u3 ②B: 1g3, 3u1p, we list out the nonzero superconductivity susceptibilities:

$$\chi_{3gt,1u} = \chi_{1u,3gt} = -\frac{\lambda_R k_F}{\sqrt{\lambda^2 + \lambda_R^2 k_F^2}} (\chi_0 + 2N\mathcal{C}_0(T, \lambda_R k_F)) \quad (31)$$

$$\chi_{3u1t,1g1} = \chi_{1g1,3u1t} = \chi_{3u2t,1g2} = \chi_{1g2,3u2t} = -\frac{\lambda_R k_F}{\sqrt{\lambda^2 + \lambda_R^2 k_F^2}} \chi_0 \quad (32)$$

$$\chi_{3u2r,1u} = \chi_{1u,3u2r} = \frac{\lambda \lambda_R k_F}{\lambda^2 + \lambda_R^2 k_F^2} (\chi_0 + 2N\mathcal{C}_0(T, \lambda_R k_F)) \quad (33)$$

$$\chi_{3u1t,3u3} = \chi_{3u3,3u1t} = -\chi_{1g2,3gr} = -\chi_{3gr,1g2} = \frac{\lambda \lambda_R k_F}{\lambda^2 + \lambda_R^2 k_F^2} \chi_0 \quad (34)$$

$$\chi_{3u2t,3gr} = \chi_{3gr,3u2t} = -\chi_{3u3,1g1} = -\chi_{1g1,3u3} = \frac{\lambda}{\sqrt{\lambda^2 + \lambda_R^2 k_F^2}} \chi_0 \quad (35)$$

$$\chi_{3u1p,1g3} = \chi_{1g3,3u1p} = \chi_{3u2r,3gt} = \chi_{3gt,3u2r} = -\frac{\lambda}{\sqrt{\lambda^2 + \lambda_R^2 k_F^2}} (\chi_0 + 2N\mathcal{C}_0(T, \lambda_R k_F)) \quad (36)$$

There are four mixing states, a. 1g1, 3u1t, 3u3; b. 1g2, 3u2t, 3gr; c. 1u, 3u2r, 3gt; d. 1g3, 3u1p. States a, b, c are A representations and state d is B representation for group $SO(2)$.

IV. FUNCTIONS FOR T_c

The critical temperature for each superconducting state is obtained by linearized gap function(Eq.(5) in the main text). We get functions for T_c s to draw phase diagram in pairing interaction parameter space.

A. First Quadrant

$$\chi_0(T_{a1}) = \frac{1}{v_0} \frac{1}{x \cos^2 \phi_F + y \sin^2 \phi_F + 1}, \quad (\Delta_{1g1}, \Delta_{3u1t}, \Delta_{3u3}) = \Delta_{a1}(1, -y \sin \phi_F, -x \cos \phi_F), \quad (37)$$

$$\chi_0(T_{b1}) = \frac{1}{v_0} \frac{1}{x \sin^2 \phi_F + y \cos^2 \phi_F + xy}, \quad (\Delta_{1g2}, \Delta_{3u2t}, \Delta_{3gr}) = \Delta_{b1}(x \sin \phi_F, -xy, -y \cos \phi_F), \quad (38)$$

$$\chi_0(T_{c1}) + 2N\mathcal{C}_0(T_{c1}, \lambda_R k_F) = \frac{1}{v_0} \frac{1}{y + x y \cos^2 \phi_F + \sin^2 \phi_F}, \quad (\Delta_{1u}, \Delta_{3u2r}, \Delta_{3gt}) = \Delta_{c1}(\sin \phi_F, x y \cos \phi_F, -y), \quad (39)$$

$$\chi_0(T_{d1}) + 2N\mathcal{C}_0(T_{d1}, \lambda_R k_F) = \frac{1}{v_0} \frac{1}{y \cos^2 \phi_F + xy}, \quad (\Delta_{1g3}, \Delta_{3u1p}) = \Delta_{d1}(x, -\cos \phi_F), \quad (40)$$

where $\phi_F = \arctan(\lambda_R k_F / \lambda)$. x, y are defined by $x = u_0/v_0 = u/v$ and $y = v/v_0 = u/u_0$. Here, we assume $\lambda_R k_F \ll \lambda$, i.e., $\phi_F \rightarrow 0$. Then, the possible pairings are reduced to only four states: 1g1, 3u2t, 3gr and 3u3. We compare these critical temperatures and get the phase diagram in the first quadrant of Fig.1c in the main text.

B. Second Quadrant

$$\chi_0(T_{a2}) = \frac{1}{v_0} \frac{1}{1 + y \sin^2 \phi_F}, \quad (\Delta_{1g1}, \Delta_{3u1t}) = \Delta_{a2}(1, -y \sin \phi_F) \quad (41)$$

$$\chi_0(T_{b2}) = \frac{1}{v_0} \frac{1}{y \cos^2 \phi_F}, \quad \Delta_{3gr} = \Delta_{b2} \quad (42)$$

$$\chi_0(T_{c2}) + 2N\mathcal{C}_0(T_{c2}, \lambda_R k_F) = \frac{1}{v_0} \frac{1}{y + \sin^2 \phi_F}, \quad (\Delta_{1u}, \Delta_{3gt}) = \Delta_{c2}(\sin \phi_F, -y) \quad (43)$$

$$\chi_0(T_{d2}) + 2N\mathcal{C}_0(T_{d2}, \lambda_R k_F) = \frac{1}{v_0} \frac{1}{y \cos^2 \phi_F}, \quad \Delta_{3u1p} = \Delta_{d2} \quad (44)$$

C. Third Quadrant

$$\chi_0(T_{a3}) = \frac{1}{v_0}, \quad \Delta_{1g1} = \Delta_{a3} \quad (45)$$

$$\chi_0(T_{b3}) = \frac{1}{v_0} \frac{1}{xy}, \quad \Delta_{3u2t} = \Delta_{b3} \quad (46)$$

$$\chi_0(T_{c3}) + 2N\mathcal{C}_0(T_{c3}, \lambda_R k_F) = \frac{1}{v_0} \frac{1}{x y \cos^2 \phi_F + \sin^2 \phi_F}, \quad (\Delta_{1u}, \Delta_{3u2r}) = \Delta_{c3}(\sin \phi_F, x y \cos \phi_F) \quad (47)$$

$$\chi_0(T_{d3}) + 2N\mathcal{C}_0(T_{d3}, \lambda_R k_F) = \frac{1}{v_0} \frac{1}{xy}, \quad \Delta_{1g3} = \Delta_{d3} \quad (48)$$

D. Fourth Quadrant

$$\chi_0(T_{a4}) = \frac{1}{v_0} \frac{1}{1 + x \cos^2 \phi_F}, \quad (\Delta_{1g1}, \Delta_{3u3}) = \Delta_{a4}(1, -x \cos \phi_F) \quad (49)$$

$$\chi_0(T_{b4}) = \frac{1}{v_0} \frac{1}{x \sin^2 \phi_F}, \quad \Delta_{1g2} = \Delta_{b4} \quad (50)$$

$$\chi_0(T_{c4}) + 2N\mathcal{C}_0(T_{c4}, \lambda_R k_F) = \frac{1}{v_0} \frac{1}{\sin^2 \phi_F}, \quad \Delta_{1u} = \Delta_{c4} \quad (51)$$

State d is absent.

V. SUPERCONDUCTIVITY WITH MAGNETIC FIELD

Consider unconventional Rashba model with Zeeman term

$$\begin{aligned} H &= H_0 + V \\ H_0 &= tk^2\sigma^0\tau^0 + \lambda\sigma^3\tau^2 \\ V &= -\lambda_R(k_y\sigma^1 - k_x\sigma^2)(\tau^0 + \tau^1) + h\sigma^3\tau^0 \end{aligned} \quad (52)$$

Solution of this Hamiltonian is carried out by perturbation method

$$E_{\alpha\beta} = tk^2 + \alpha\lambda + \beta\sqrt{\lambda_R^2 k^2 + h^2}, \quad \alpha, \beta \in \{+, -\} \quad (53)$$

The unitary matrix to approximately diagonalize H is

$$U = \frac{1}{\sqrt{2}} \begin{pmatrix} -i\cos\frac{\varphi}{2} & -i\sin\frac{\varphi}{2} & i\cos\frac{\varphi}{2} & i\sin\frac{\varphi}{2} \\ ie^{i\theta}\sin\frac{\varphi}{2} & -ie^{i\theta}\cos\frac{\varphi}{2} & ie^{i\theta}\sin\frac{\varphi}{2} & -ie^{i\theta}\cos\frac{\varphi}{2} \\ \cos\frac{\varphi}{2} & \sin\frac{\varphi}{2} & \cos\frac{\varphi}{2} & \sin\frac{\varphi}{2} \\ e^{i\theta}\sin\frac{\varphi}{2} & -e^{i\theta}\cos\frac{\varphi}{2} & -e^{i\theta}\sin\frac{\varphi}{2} & e^{i\theta}\cos\frac{\varphi}{2} \end{pmatrix} \quad (54)$$

where $\varphi = \arctan(\lambda_R k/h)$. Thus Green function for electron is

$$\begin{aligned} G^0(\mathbf{k}, i\omega_n) &= G_{++++}\sigma^0\tau^0 + G_{+---}\sigma^3\tau^2 + G_{+-+-} \left(\frac{\lambda_R k}{\sqrt{\lambda_R^2 k^2 + h^2}} |\mathbf{k} \times \boldsymbol{\sigma}|_z \tau^1 \right. \\ &\quad \left. + \frac{h}{\sqrt{\lambda_R^2 k^2 + h^2}} \sigma^3\tau^0 \right) + G_{+-+} \left(\frac{h}{\sqrt{\lambda_R^2 k^2 + h^2}} \sigma^0\tau^2 - \frac{\lambda_R k}{\sqrt{\lambda_R^2 k^2 + h^2}} (\mathbf{k} \cdot \boldsymbol{\sigma})\tau^3 \right) \end{aligned} \quad (55)$$

where $G_{\alpha\beta\gamma\delta} = (\alpha\tilde{G}_{++} + \beta\tilde{G}_{+-} + \gamma\tilde{G}_{-+} + \delta\tilde{G}_{--})/4$, $\tilde{G}_{\alpha\beta}(\mathbf{k}, i\omega_n) = 1/(i\omega_n - E_{\alpha\beta})$. And we find $g_{\mu\nu\rho\sigma}^{\alpha\beta\gamma\delta}$ s are different from the ones in Section III.

$$\begin{aligned} g_{++++}^{++++} &= g_{+---}^{+---} = -g_{++--}^{++--} = -g_{+-+-}^{+-+-} = \frac{1}{8}\chi_0 + \frac{1}{8}N\mathcal{C}_0(T, \sqrt{\lambda_R^2 k_F^2 + h^2}) \\ g_{+-+}^{+-+-} &= g_{+--+}^{+--+} = -g_{+-+}^{+-+} = -g_{+-+}^{+-+} = -\frac{1}{8}N\mathcal{C}_0(T, \sqrt{\lambda_R^2 k_F^2 + h^2}) \end{aligned}$$

The self-superconductivity-susceptibilities are

$$\chi_{1g1,1g1} = \chi_{3u3,3u3} = \chi_0 + \frac{h^2}{\lambda_R^2 k_F^2 + h^2} 2N\mathcal{C}_0(T, \sqrt{\lambda_R^2 k_F^2 + h^2}) \quad (56)$$

$$\chi_{3u2r,3u2r} = \chi_{3gt,3gt} = \chi_0 + \frac{\lambda_R^2 k_F^2}{\lambda_R^2 k_F^2 + h^2} 2N\mathcal{C}_0(T, \sqrt{\lambda_R^2 k_F^2 + h^2}) \quad (57)$$

$$\chi_{3u2t,3u2t} = \chi_{3gr,3gr} = \chi_0 \quad (58)$$

$$\chi_{1g3,1g3} = \chi_{3u1p,3u1p} = \chi_0 + 2N\mathcal{C}_0(T, \sqrt{\lambda_R^2 k_F^2 + h^2}) \quad (59)$$

The nonzero inter-superconductivity-susceptibilities of possible mixing states are

$$\chi_{1g1,3u2r} = \chi_{3u3,3gt} = -\chi_{3u2r,1g1} = -\chi_{3gt,3u3} = -i \frac{h\lambda_R k_F}{\lambda_R^2 k_F^2 + h^2} 2N\mathcal{C}_0(T, \sqrt{\lambda_R^2 k_F^2 + h^2}) \quad (60)$$

$$\chi_{1g1,3gt} = \chi_{3u3,3u2r} = -\chi_{3gt,1g1} = -\chi_{3u2r,3u3} = i \frac{h\lambda_R k_F}{\lambda_R^2 k_F^2 + h^2} 2N\mathcal{C}_0(T, \sqrt{\lambda_R^2 k_F^2 + h^2}) \quad (61)$$

$$\chi_{1g1,3u3} = \chi_{3u3,1g1} = -[\chi_0 + \frac{h^2}{\lambda_R^2 k_F^2 + h^2} 2N\mathcal{C}_0(T, \sqrt{\lambda_R^2 k_F^2 + h^2})] \quad (62)$$

$$\chi_{3u2r,3gt} = \chi_{3gt,3u2r} = -[\chi_0 + \frac{\lambda_R^2 k_F^2}{\lambda_R^2 k_F^2 + h^2} 2N\mathcal{C}_0(T, \sqrt{\lambda_R^2 k_F^2 + h^2})] \quad (63)$$

$$\chi_{3u2t,3gr} = \chi_{3gr,3u2t} = \chi_0 \quad (64)$$

$$\chi_{1g3,3u1p} = \chi_{3u1p,1g3} = -[\chi_0 + 2N\mathcal{C}_0(T, \sqrt{\lambda_R^2 k_F^2 + h^2})] \quad (65)$$

There remain three mixing states, \mathcal{A} . 1g1, 3u2r, 3gt, 3u3; \mathcal{B} . 3u2t, 3gr; \mathcal{D} . 1g3, 3u1p. States \mathcal{A} , \mathcal{B} are A representations and state \mathcal{D} is B representation for group $SO(2)$. We notice state \mathcal{A} is the combination of states a and c for zero field case.

A. First Quadrant

In the first quadrant, we get the critical temperatures

$$\chi_0(T_{\mathcal{A}1}) + \mathcal{C}_0 = \frac{1}{2v_0(1+x)y} \{1 + y - \sqrt{4v_0^2(1+x)^2y^2\mathcal{C}_0^2 + 4v_0(1+x)(1-y)\cos 2\varphi\mathcal{C}_0 + (1-y)^2}\} \quad (66)$$

$$\chi_0(T_{\mathcal{B}1}) = \frac{1}{v_0(1+x)y} \quad (67)$$

$$\chi_0(T_{\mathcal{D}1}) + 2\mathcal{C}_0 = \frac{1}{v_0(1+x)y} \quad (68)$$

where $\mathcal{C}_0 = N\mathcal{C}_0(T, \lambda_R k_F, h)$. We find the state \mathcal{B} is not affected by the magnetic field, while states \mathcal{A} and \mathcal{D} are affected differently. To investigate the difference of \mathcal{A} and \mathcal{D} , one could make a subtraction between Eq.(66,68)

$$2\ln\left(\frac{T_{\mathcal{D}1}}{T_{\mathcal{A}1}}\right) = \mathcal{C}_0 - \frac{1}{2v_0(1+x)y} \{1 - y + \sqrt{4v_0^2(1+x)^2y^2\mathcal{C}_0^2 + 4v_0(1+x)(1-y)\cos 2\varphi\mathcal{C}_0 + (1-y)^2}\} \quad (69)$$

If we want $T_{\mathcal{D}1} > T_{\mathcal{A}1}$, parameters should obey $\{1/[1 + 2v_0(1+x)\mathcal{C}_0], -\cos 2\varphi\}_{max} < y < 1$, however the situation could never be satisfied since $\mathcal{C}_0 < 0$. Therefore state \mathcal{D} is not affected less by magnetic field than state \mathcal{A} . The similar results could be obtained for the other quadrants.

B. Second Quadrant

$$\chi_0(T_{\mathcal{A}2}) + \mathcal{C}_0 = \frac{1}{2v_0y} \{1 + y - \sqrt{4v_0^2y^2\mathcal{C}_0^2 + 4v_0y(1-y)\cos 2\varphi\mathcal{C}_0 + (1-y)^2}\}, \quad (\Delta_{1g1}, \Delta_{3gt}) \quad (70)$$

$$\chi_0(T_{\mathcal{B}2}) = \frac{1}{v_0y}, \quad \Delta_{3gr} \quad (71)$$

$$\chi_0(T_{\mathcal{D}2}) + 2\mathcal{C}_0 = \frac{1}{v_0y}, \quad \Delta_{3u1p} \quad (72)$$

C. Third Quadrant

$$\chi_0(T_{\mathcal{A}3}) + \mathcal{C}_0 = \frac{1}{2v_0xy} \{1 + xy - \sqrt{4v_0^2x^2y^2\mathcal{C}_0^2 + 4v_0xy(1-xy)\cos 2\varphi\mathcal{C}_0 + (1-xy)^2}\}, \quad (\Delta_{1g1}, \Delta_{3u2r}) \quad (73)$$

$$\chi_0(T_{\mathcal{B}3}) = \frac{1}{v_0xy}, \quad \Delta_{3u2t} \quad (74)$$

$$\chi_0(T_{\mathcal{D}3}) + 2\mathcal{C}_0 = \frac{1}{v_0xy}, \quad \Delta_{1g3} \quad (75)$$

D. Fourth Quadrant

$$\chi_0(T_{\mathcal{A}4}) + 2\cos^2\varphi\mathcal{C}_0 = \frac{1}{v_0(1+x)}, \quad (\Delta_{1g1}, \Delta_{3u3}) \quad (76)$$

States \mathcal{B} and \mathcal{D} are absent in this situation.

VI. TUNNELING PROCESS

To get the information of the interaction parameters, we find a way to detect which one of the two p-wave triplet state is leading. The eigenstates of quasi-particles are solutions of the 8×8 Bogoliubov-de Gennes(BdG) Hamiltonian(77) in Nambu space ($c_{\mathbf{k},1\uparrow}^\dagger, c_{\mathbf{k},1\downarrow}^\dagger, c_{\mathbf{k},2\uparrow}^\dagger, c_{\mathbf{k},2\downarrow}^\dagger, c_{-\mathbf{k},1\uparrow}, c_{-\mathbf{k},1\downarrow}, c_{-\mathbf{k},2\uparrow}, c_{-\mathbf{k},2\downarrow}$), which have tedious spinor that make the tunneling problem difficult to solve, especially for the state 3gr.

$$H_{BdG}(\mathbf{k}) = \begin{pmatrix} H_0(\mathbf{k}) & \Delta(\mathbf{k}) \\ \Delta^\dagger(\mathbf{k}) & -H_0^T(-\mathbf{k}) \end{pmatrix} \quad (77)$$

Fortunately, the upper two bands affect little to the lower bands as $\lambda_R k_F \ll \lambda$, therefore we would make a downfolding approach and get an effective 4×4 BdG Hamiltonian. We firstly make a rotation in the spinor space.

$$\tilde{H}_{BdG} = \begin{pmatrix} U_r^\dagger & \\ & U_r \end{pmatrix} H_{BdG} \begin{pmatrix} U_r & \\ & U_r^\dagger \end{pmatrix} = \begin{pmatrix} \tilde{H}_0(\mathbf{k}) & \tilde{\Delta}(\mathbf{k}) \\ \tilde{\Delta}^\dagger(\mathbf{k}) & -\tilde{H}_0^T(-\mathbf{k}) \end{pmatrix} \quad (78)$$

Here $U_r = (\sigma^0 \tau^0 + i \sigma^3 \tau^1) / \sqrt{2}$, and thus parameter λ goes into diagonal elements of the matrix. The block elements are listed below, superconducting states for 1g1, 3u2t and 3gr are considered.

$$\tilde{H}_0(\mathbf{k}) = \xi_{\mathbf{k}} \sigma^0 \tau^0 - \lambda_R (k_x \sigma^1 + k_y \sigma^2) (\tau^0 + \tau^1) + \lambda \sigma^0 \tau^3 \quad (79)$$

$$\tilde{\Delta}^{1g1}(\mathbf{k}) = i \Delta \sigma^2 \tau^0 \quad (80)$$

$$\tilde{\Delta}^{3u2t}(\mathbf{k}) = \Delta (k_x \sigma^3 \tau^0 - i k_y \sigma^0 \tau^0) \quad (81)$$

$$\tilde{\Delta}^{3gr}(\mathbf{k}) = \Delta (-k_x \sigma^3 \tau^3 + i k_y \sigma^0 \tau^3) \quad (82)$$

After rearranging the basis in $(c_{\mathbf{k},+1\uparrow}^\dagger, c_{\mathbf{k},+1\downarrow}^\dagger, c_{-\mathbf{k},+1\uparrow}, c_{-\mathbf{k},+1\downarrow}, c_{\mathbf{k},-1\uparrow}^\dagger, c_{\mathbf{k},-1\downarrow}^\dagger, c_{-\mathbf{k},-1\uparrow}, c_{-\mathbf{k},-1\downarrow})$, where + and - denote combinations of orbitals that have diagonal elements $\xi_{\mathbf{k}} + \lambda$ and $\xi_{\mathbf{k}} - \lambda$, we get the Hamiltonian in form of

$$\tilde{H}_{BdG}^r = \begin{pmatrix} \hat{h}^+ + \hat{\Delta}^+ & T \\ T^\dagger & \hat{h}^- + \hat{\Delta}^- \end{pmatrix} \quad (83)$$

The elements in Eq.(83) are

$$\hat{h}^\pm = \hat{h}_0^\pm + \hat{h}_R, \quad \hat{h}_0^\pm = (\xi_{\mathbf{k}} \pm \lambda) \sigma^0 \eta^3, \quad \hat{h}_R = -\lambda_R (k_x \sigma^1 \eta^0 + k_y \sigma^2 \eta^3) \quad (84)$$

$$\hat{\Delta}_{1g1}^+ = \hat{\Delta}_{1g1}^- = -\Delta \sigma^2 \eta^2 \quad (85)$$

$$\hat{\Delta}_{3u2t}^+ = \hat{\Delta}_{3u2t}^- = -\hat{\Delta}_{3gr}^+ = \hat{\Delta}_{3gr}^- = \Delta (k_x \sigma^3 \eta^1 + k_y \sigma^0 \eta^2) \quad (86)$$

$$T = -\lambda_R (k_x \sigma^1 \eta^0 + k_y \sigma^2 \eta^3) \quad (87)$$

Pauli matrices (η^0, η) span the particle-hole space. Then use the downfolding approach, and find the effective BdG Hamiltonian for the lower bands.

$$\begin{aligned} \hat{H}_{BdG}^{eff} &\approx \hat{h}^- + \hat{\Delta}^- - T^\dagger (\hat{h}^+ + \hat{\Delta}^+)^{-1} T \\ &\approx \hat{h}^- + \hat{\Delta}^- + \delta \hat{h} \end{aligned} \quad (88)$$

$\delta \hat{h}$ describes the influence from the upper bands, which is different from states.

$$\delta \hat{h}^{1g1} = -\frac{\lambda_R^2 k^2}{2\lambda} [(u_\lambda^2 - v_\lambda^2) \sigma^0 \eta^3 + 2u_\lambda v_\lambda \sigma^2 \eta^2] \quad (89)$$

$$\delta \hat{h}^\nu = \frac{\lambda_R^2 k}{2\lambda} [(v_\lambda^2 - u_\lambda^2) k \sigma^0 \eta^3 + 2\nu u_\lambda v_\lambda (k_x \sigma^3 \eta^1 + k_y \sigma^0 \eta^2)] \quad (90)$$

$\nu = +1(-1)$ denotes states 3u2t(3gr), $u(v)_\lambda^2 = (\sqrt{(2\lambda)^2 + \Delta^2} + (-)2\lambda)/2\sqrt{(2\lambda)^2 + \Delta^2}$. Positive eigenenergys and corresponding eigenstates of the effective Hamiltonian(88) have compact form.

$$E_\pm^\nu = \sqrt{(\xi_{\mathbf{k}} - \lambda \pm \lambda_R k - \epsilon_0 \cos 2\gamma)^2 + (\Delta + \nu \epsilon_0 \sin 2\gamma)^2} \quad \psi_\pm^\nu = (\pm u_\nu, -e^{i\theta} u_\nu, \pm e^{i\theta} v_\nu, v_\nu) \quad (91)$$

$$E_\pm^{1g1} = E_\pm^1 \quad \psi_\pm^{1g1} = (u_1, \mp e^{i\theta} u_1, \pm e^{i\theta} v_1, v_1) \quad (92)$$

Here $\gamma = \arctan(v_\lambda/u_\lambda)$, $\epsilon_0 = \lambda_R^2 k^2 / 2\lambda$, in tunneling problem $u(v)_\nu^2 = (E + (-)\sqrt{E^2 - (\Delta + \nu\epsilon_0 \sin 2\gamma)^2})/2E$ for the given energy E .

Then we solve Eq.(9) in the main text. Supposing the condition $(\lambda_R k_F, \sqrt{E^2 - \Delta^2}) \ll \mu$ as μ is the same order comparing with λ , wave vectors of the normal metal electron and BdG quasi-particle states are approximately the same and equal to $k_F = \sqrt{2m\mu}/\hbar$. Since the unconventional Rashba bands have infinitesimal spin structures as $\lambda_R k_F \ll \lambda$, conductance would not be differed by spin, thus we arbitrarily choose a spin-up incident electron. The wave function for region $x < 0$ is

$$\psi_L(x) = e^{ik_y y} \begin{bmatrix} 1 \\ 0 \\ 0 \\ 0 \end{bmatrix} + b_{11} e^{-ik_x x} \begin{bmatrix} 1 \\ 0 \\ 0 \\ 0 \end{bmatrix} + b_{12} e^{-ik_x x} \begin{bmatrix} 0 \\ 1 \\ 0 \\ 0 \end{bmatrix} + a_{11} e^{ik_x x} \begin{bmatrix} 0 \\ 0 \\ 1 \\ 0 \end{bmatrix} + a_{12} e^{ik_x x} \begin{bmatrix} 0 \\ 0 \\ 0 \\ 1 \end{bmatrix} \quad (93)$$

For 3u2t or 3gr, the wave function for region $x > 0$ is

$$\psi_R^\nu(x) = \frac{1}{\sqrt{2}} e^{ik_y y} [c_{11} e^{ik_x x} \begin{bmatrix} u_\nu \\ -e^{i\theta} u_\nu \\ e^{i\theta} v_\nu \\ v_\nu \end{bmatrix} + c_{12} e^{ik_x x} \begin{bmatrix} -u_\nu \\ -e^{i\theta} u_\nu \\ -e^{i\theta} v_\nu \\ v_\nu \end{bmatrix} + d_{11} e^{-ik_x x} \begin{bmatrix} v_\nu \\ e^{-i\theta} v_\nu \\ -e^{-i\theta} u_\nu \\ u_\nu \end{bmatrix} + d_{12} e^{-ik_x x} \begin{bmatrix} -v_\nu \\ e^{-i\theta} v_\nu \\ e^{-i\theta} u_\nu \\ u_\nu \end{bmatrix}] \quad (94)$$

Terms after coefficients 'c's are electron-like quasiparticle transmissions and terms after 'd's are hole-like quasiparticle transmissions. The coefficients a,b,c,d are determined by equations:

$$\psi_L(0^-) = \psi_R(0^+) \quad (95)$$

$$\frac{d\psi_R}{dx}|_{0^+} - \frac{d\psi_L}{dx}|_{0^-} = \frac{2mU_0}{\hbar^2} \psi(0) \quad (96)$$

The results are

$$a_{11} = \frac{4e^{i\theta} u_\nu v_\nu}{(4 + Z^2)u_\nu^2 + e^{2i\theta} Z^2 v_\nu^2} \quad (97)$$

$$a_{12} = 0 \quad (98)$$

$$b_{11} = -\frac{(u_\nu^2 + e^{2i\theta} v_\nu^2)Z(Z + 2i)}{(4 + Z^2)u_\nu^2 + e^{2i\theta} Z^2 v_\nu^2} \quad (99)$$

$$b_{12} = 0 \quad (100)$$

$$c_{11} = -\frac{i\sqrt{2}u_\nu(Z + 2i)}{(4 + Z^2)u_\nu^2 + e^{2i\theta} Z^2 v_\nu^2} \quad (101)$$

$$c_{12} = \frac{i\sqrt{2}u_\nu(Z + 2i)}{(4 + Z^2)u_\nu^2 + e^{2i\theta} Z^2 v_\nu^2} \quad (102)$$

$$d_{11} = -\frac{i\sqrt{2}e^{2i\theta} v_\nu Z}{(4 + Z^2)u_\nu^2 + e^{2i\theta} Z^2 v_\nu^2} \quad (103)$$

$$d_{12} = \frac{i\sqrt{2}e^{2i\theta} v_\nu Z}{(4 + Z^2)u_\nu^2 + e^{2i\theta} Z^2 v_\nu^2} \quad (104)$$

We also get the coefficients for 1g1

$$a_{11} = 0 \quad (105)$$

$$a_{12} = \frac{4u_1 v_1}{(4 + Z^2)u_1^2 - Z^2 v_1^2} \quad (106)$$

$$b_{11} = -\frac{(u_1^2 - v_1^2)Z(Z + 2i)}{(4 + Z^2)u_1^2 - Z^2 v_1^2} \quad (107)$$

$$b_{12} = 0 \quad (108)$$

$$c_{11} = c_{12} = -\frac{i\sqrt{2}u_1(Z + 2i)}{(4 + Z^2)u_1^2 - Z^2 v_1^2} \quad (109)$$

$$d_{11} = d_{12} = \frac{i\sqrt{2}v_1 Z}{(4 + Z^2)u_1^2 - Z^2 v_1^2} \quad (110)$$

where $Z = 2mU_0/\hbar^2k_F$. The tunneling conductance normalized by normal state is

$$G = \frac{1}{2} \int_{-\pi/2}^{\pi/2} d\theta \cos\theta (1 + |a_{11}|^2 + |a_{12}|^2 - |b_{11}|^2 - |b_{12}|^2) \quad (111)$$
